# Color-Octet Contributions to Inelastic Heavy-Quarkonium Production

Jungil Lee

II. Institut für Theoretische Physik, Universität Hamburg, 22761 Hamburg, Germany

**Abstract.** The color-octet mechanism based on the nonrelativistic QCD (NRQCD) factorization approach in inclusive heavy quarkonium production in high energy processes is reviewed. As phenomenological applications, we discuss charmonium production at HERA and $\Upsilon$ production associated with weak gauge bosons at the LHC.

## 1 Introduction

In high energy experiments, $J^{PC} = 1^{--}$ quarkonium states, such as the charmonium state $J/\psi$ and the bottonium state $\Upsilon$, have been used as clean probes to study QCD. They provide an enormous suppression of the backgrounds due to their leptonic decay modes. For a long time, the color singlet model (CSM) [1,2] has been a reasonable picture to describe heavy quarkonium production and decay. The CSM allows for a color-singlet heavy quark pair to form a quarkonium system in the same spectroscopic state $^{2S+1}L_J$. Factorization of the short distance process from bound state formation is assumed due to the separation of the two scales governing them. The short distance process is calculated in perturbative QCD, and the wavefunction and its derivatives at the origin, which involve nonperturbative physics, are calculated within potential models or phenomenological analyses.

In the middle of the 1990's, serious discrepancies between several experimental results and the CSM were found, and this naive factorization approach was reexamined. For example, the dominant mechanism of large $p_T$ $J/\psi$ production in $p\overline{p}$ collisions, has been found to be parton fragmentation in the framework of the CSM, by Braaten and Yuan [3]. This fragmentation mechanism has been applied to various studies on prompt charmonium production at the Tevatron [4], and the CDF data on prompt $J/\psi$ production [5] qualitatively meet these theoretical predictions. This fragmentation picture in the CSM was not enough. The $\psi'$ production rate measured by CDF was 30 times larger than the theoretical prediction even after including the parton fragmentation mechanism, which is the so-called $\psi'$ anomaly [6]. Based on NRQCD, Braaten and Fleming proposed the color-octet gluon fragmentation picture as a possible scenario to resolve this problem [7]. They included gluon fragmentation into a color-octet $Q\overline{Q}$ pair in the $^3S_1^{(8)}$ state followed by the soft transition of this pair into physical quarkonium. This subprocess is not allowed in the CSM, where only the color-singlet $Q\overline{Q}$ pair in the same spectroscopic state ($^3S_1^{(1)}$) corresponding to the final-state quarkonium can be hadronized into that quarkonium. As an effective

field theory of QCD, NRQCD [8,9] was developed to describe heavy quarkonium production and decay in a rigorous way from the first principles of QCD. In NRQCD, it is allowed to make a quarkonium state from various $Q\overline{Q}$'s with color and spin states which need not be the same as those of the final quarkonium state. Among an infinite number of channels, only a few channels dominate the soft transition process, as may be seen with the help of NRQCD velocity scaling rules [8,9]. Newly introduced nonperturbative NRQCD matrix elements should then be fixed from experimental data. Efforts are being made to extract the NRQCD matrix elements from experiments to test universality.

This talk is organized as follows. We first review the basics of NRQCD in the analysis of the inclusive production of heavy quarkonium. Then we discuss charmonium production at HERA and associate production of $\Upsilon$ and weak gauge bosons at the LHC.

## 2 NRQCD Basics

### 2.1 Lagrangian

By use of the mass splitting of heavy quarkonia, one may assume the velocity $v$ of the heavy quark inside the system to be small, and therefore one finds the separation among the three important scales, heavy quark mass $M$, momentum in meson rest frame $Mv$ and binding energy $Mv^2$ as

$$M \gg Mv \gg Mv^2 \quad \text{where} \quad v_b^2 \sim 0.1, \quad v_c^2 \sim 0.3. \tag{1}$$

The NRQCD Lagrangian is obtained from full QCD by introducing an ultravio-

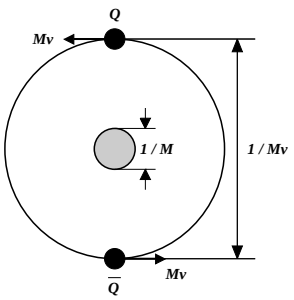


**Fig. 1.** Typical scales of a heavy quarkonium system.

let momentum cutoff $\Lambda$ that is of order $M$, since the important nonperturbative physics involves momenta of order $Mv$ or less. One can compensate the removal of the relativistic states by adding local interactions to the Lagrangian order by order in $1/M$. Due to the decoupling of particle and antiparticle in this region, the dynamics of the heavy quarks can be described in nonrelativistic Schrödinger

field theory. Only the heavy quark part is modified from the full QCD Lagrangian [8,9]:

$$\mathcal{L} = \mathcal{L}_{\rm light} + \mathcal{L}_{\rm heavy} + \delta\mathcal{L}, \tag{2}$$

$$\mathcal{L}_{\rm heavy} = \psi^\dagger \left( iD_t + \frac{\boldsymbol{D}^2}{2M} \right) \psi + \chi^\dagger \left( iD_t - \frac{\boldsymbol{D}^2}{2M} \right) \chi. \tag{3}$$

In LO ($\delta\mathcal{L} = 0$), there is no spin-flip operator and this leads to *approximate* heavy quark spin symmetry (HQSS) of NRQCD. The LO NRQCD Lagrangian naturally allows for a color-octet term via the chromoelectric dipole (E1) transition which is included in $\boldsymbol{D}^2/(2M)$. The relativistic effects from full QCD are included in the correction term $\delta\mathcal{L}$. The correction term is composed of bilinear terms

$$\begin{aligned} \delta\mathcal{L}_{\rm bilinear} = & \frac{c_1}{8M^3} \left( \psi^\dagger (\mathbf{D}^2)^2 \psi \; - \; \chi^\dagger (\mathbf{D}^2)^2 \chi \right) + \cdots \\ & + \frac{c_4}{2M} \left( \psi^\dagger (g\mathbf{B}\cdot\boldsymbol{\sigma}) \psi \; - \; \chi^\dagger (g\mathbf{B}\cdot\boldsymbol{\sigma}) \chi \right), \end{aligned} \tag{4}$$

which describe further details of low energy physics, and four-fermion interaction terms

$$\delta\mathcal{L}_{4-\rm fermion} = \sum_n \left[ \frac{f_n(\Lambda)}{M^{d_n-4}} \psi^\dagger \Gamma_n \chi \chi^\dagger \Gamma_n' \psi + \frac{f_n^{EM}(\Lambda)}{M^{d_n-4}} \psi^\dagger \Gamma_n \chi |0\rangle\langle 0| \chi^\dagger \Gamma_n' \psi \right]. \tag{5}$$

The former represent the heavy quark pair annihilation into light hadrons while the latter describe the electromagnetic annihilation in NRQCD. The short distance scale physics is included in the coefficient $f_n^{EM}$. The bilinear part includes all the higher dimensional operators coming from the expansion in the heavy quark velocity $v$. Here we find the spin-flip operator $\boldsymbol{\sigma}$ in the chromomagnetic dipole (M1) transition.

### 2.2 Velocity Scaling Rules

The velocity scaling rules [8,9] classify the importance of each term in the NRQCD interaction Lagrangian in powers of $v_Q^2$. For example, the most important channels of $J/\psi$ production can be classified as

$$\begin{aligned} & (c\overline{c})({}^3S_1^{(8)}) \to J/\psi : (E1)^2 : v^4 \times (c\overline{c})({}^3S_1^{(1)} \to J/\psi), \\ & (c\overline{c})({}^1S_0^{(8)}) \to J/\psi : (M1)^1 : v^3 \times (c\overline{c})({}^3S_1^{(1)} \to J/\psi), \\ & (c\overline{c})({}^3P_J^{(8)}) \to J/\psi : (E1)^1 : v^4 \times (c\overline{c})({}^3S_1^{(1)} \to J/\psi). \end{aligned} \tag{6}$$

Note that ${}^3P_J^{(8)}$ is further suppressed by $v^2$ in addition to the E1 transition factor $v^2$, since the operator itself has a covariant derivative. If we only consider the long distance part, the color singlet matrix element dominates over the color octet ones. Therefore the color octet mechanism dominates over the color singlet channel only when the short distance coefficient for the octet channel is large enough to compensate the suppression in the long distance factor.

### 2.3 Factorization and Matching in Inclusive Heavy Quarkonium Production

Factorization in the inclusive heavy quarkonium production rate comes from the idea that the probability of forming a bound state from a heavy quark pair produced in a short distance process is significant only if the corresponding production points are separated by a distance of order $1/M$ or less [9]. Then the production rate of the heavy quark pair within a distance scale of order $1/M$ is factored out from the formation of the bound state with distance scale of order $1/(Mv)$ or larger. The latter is accurately described by NRQCD. The vacuum expectation value of a four-quark operator describes the transition rate of the long distance process.

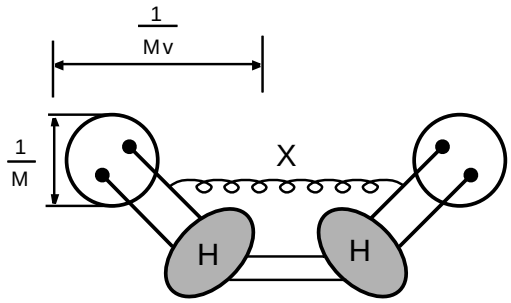


**Fig. 2.** Diagram representing the NRQCD color octet matrix element.

As shown in Fig.2, the operator creates the heavy quark pair at a spacetime point and propagates into the asymptotic future, where the final state includes the heavy quarkonium state, and then propagates back to the creation point. The factorization formula of inclusive quarkonium $H$ production is then given by [9]

$$\sigma(H) \;=\; \sum_n \frac{F_n(\Lambda)}{M^{d_n-4}} \,\langle 0|\mathcal{O}_n^H(\Lambda)|0\rangle, \tag{7}$$

where $F_n$ is the short distance coefficient, which is infrared and collinear finite, and $\mathcal{O}_n^H$ is the four-quark operator of the inclusive production mentioned above. The factorization scale $\Lambda$ is of order of the heavy quark mass $M$. The most

important operators in $1^{--}$ quarkonium production are given by

$$\begin{aligned}
\mathcal{O}_1^H(^3S_1) &= \chi^\dagger\sigma^i\psi\left(a_H^\dagger a_H\right)\psi^\dagger\sigma^i\chi, \\
\mathcal{O}_8^H(^1S_0) &= \chi^\dagger T^a\psi\left(a_H^\dagger a_H\right)\psi^\dagger T^a\chi, \\
\mathcal{O}_8^H(^3S_1) &= \chi^\dagger\sigma^i T^a\psi\left(a_H^\dagger a_H\right)\psi^\dagger\sigma^i T^a\chi, \\
\mathcal{O}_8^H(^3P_0) &= \frac{1}{3}\chi^\dagger\sigma^i D^i T^a\psi\left(a_H^\dagger a_H\right)\psi^\dagger\sigma^j D^j T^a\chi, \\
a_H^\dagger a_H \quad &\equiv \sum_X\sum_{m_J}|H+X\rangle\langle H+X|,
\end{aligned} \tag{8}$$

where the sums are over the spin states of $H$ and over all other final states. The scale dependence of each matrix element is canceled after summing over all the contributions. Expanding the perturbative QCD amplitude in $v$, one can find out the partial wave amplitudes with NRQCD operators. In this matching procedure, one can extract the short distance coefficients $F_n$.

## 3 Quarkonium Production at HERA

After the color-octet mechanism was applied to high $p_T$ $\psi'$ production via gluon fragmentation at the Tevatron [7], studies of $J/\psi$ production including the color-octet mechanism were activated. Cho and Leibovich considered a large class of color-octet diagrams which can contribute to $J/\psi$ production at hadron colliders [10], below the region where fragmentation is dominant. The same approach has been used in inclusive photoproduction of $J/\psi$ [11,12]. In the region where gluon fragmentation does not dominate, two more NRQCD color-octet matrix elements, $\langle\mathcal{O}_8^{J/\psi}(^1S_0)\rangle$ and $\langle\mathcal{O}_8^{J/\psi}(^3P_0)\rangle$, contribute significantly. Unfortunately, they appear in a linear combination, and this makes it difficult to determine their numerical values separately. Furthermore, the results obtained from the Tevatron data [10] are not appropriate to explain the photoproduction data [11,12]. The energy distribution of the produced $J/\psi$ meson is one of the most important measurable quantities in this process. While the CSM is enough to explain the data in the lower $z$ region [13,14] ($z$ is the $J/\psi$ energy fraction of the initial photon in the proton rest frame), the data in the higher $z$ region region ($z < 0.8 \sim 0.9$), where color-octet contribution is suppressed, was not well explained. The diverging behavior of the contribution in the higher $z$ region due to the color-octet mechanism seemed to be troublesome. However, Beneke, Rothstein and Wise showed that the NRQCD expansion may lead to a breakdown near the boundaries of phase space [15]. Further analysis on this end point region dynamics would give a clearer explanation of the $J/\psi$ energy distribution in the high $z$ region. Fleming and Mehen [16] suggested that the leptoproduction analysis could avoid the end point region ambiguity. In the high $Q^2$ region of leptoproduction, the corrections coming from the non-relativistic approximation of the quarkonium phase space become negligible [16]. They also predicted the

polarization of $J/\psi$ in leptoproduction. But the data sample is not sufficient to confirm their predictions yet [17]. Recently, Kniehl and Kramer took into account HO QCD effects [18] due to the multiple emission of gluons, which had been estimated by Monte Carlo techniques [19]. As a consequence, the excess of the NRQCD prediction at $z$ close to unity over the HERA data disappeared. So, the complete NLO analysis on this process is called for.

## 4 $pp \to \Upsilon + W/Z + X$

The associated production of a $W^{\pm}$ or $Z^0$ boson and a $J/\psi$ meson has been studied previously, but only for $J/\psi$'s with large transverse momentum, where the process is dominated by gluon fragmentation into $J/\psi$ [20]. The differential cross sections for $W^{\pm} + J/\psi$ and $Z^0 + J/\psi$ peak at small transverse momentum of the $J/\psi$. Because the mass of the $\Upsilon$ is larger than that of the $J/\psi$ by a factor of 3, the cross sections for $W^{\pm} + \Upsilon$ and $Z^0 + \Upsilon$ are much smaller than those for $W^{\pm} + J/\psi$ and $Z^0 + J/\psi$. However the larger mass of the $\Upsilon$ makes it possible to observe the leptons from its decay, even if the $\Upsilon$ is produced at small transverse momentum. It is therefore possible to measure the total cross sections for $W^{\pm} + \Upsilon$ and $Z^0 + \Upsilon$.

Let us consider the production of $W^{\pm}/Z + \Upsilon$ at a hadron collider. The $2 \to 3$ parton processes that produce $W^+/Z + b\bar{b}$ are shown in Fig.3. The cross sections

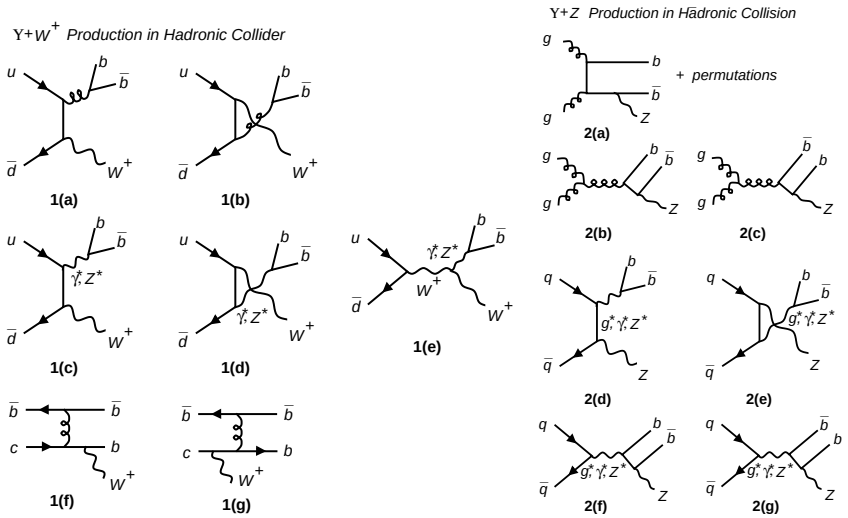


**Fig. 3.** $2 \to 3$ parton processes that produce $W^+/Z + b\bar{b}$.

for the production of $W^{\pm} + \Upsilon$ and $Z^0 + \Upsilon$ in $pp$ collisions at the LHC with

center-of-mass energy 14 TeV are [21]

$$\sum_{\pm} \sigma(W^{\pm} + \Upsilon) = 10 \text{ fb } \frac{\sum B\langle \mathcal{O}_1(^3S_1)\rangle}{8 \text{ GeV}^3} + 4000 \text{ fb } \frac{\sum B\langle \mathcal{O}_8(^3S_1)\rangle}{0.4 \text{ GeV}^3}, \quad (9)$$

$$\sigma(Z^0 + \Upsilon) = 500 \text{ fb } \frac{\sum B\langle \mathcal{O}_1(^3S_1)\rangle}{8 \text{ GeV}^3} + 1300 \text{ fb } \frac{\sum B\langle \mathcal{O}_8(^3S_1)\rangle}{0.4 \text{ GeV}^3}. \quad (10)$$

where $\sum B\langle \mathcal{O}_{1,8}(^3S_1)\rangle$ includes the feed-down processes from higher bottonium states as well as direct production of $\Upsilon$. Their numerical values are estimated [21] as shown in the denominator. The leading order GRV-94 parton distributions are used, and the factorization and renormalization scales are set equal. We neglect the masses of the $u$, $d$, $s$, and $c$ quarks, and we use the value 4.7 GeV for the $b$ quark mass. The theoretical error due to unknown higher order perturbative corrections can be estimated by varying the factorization and renormalization scales by a factor of 2 and is roughly 35%. The theoretical error due to the uncertainty in the $b$ quark mass can be estimated by varying $m_b$ by 0.25 GeV and is roughly 25%. With an integrated luminosity of 10 fb$^{-1}$, the number of events in the purely leptonic decay channels should be about 440 for $W^{\pm} + \Upsilon$ and about 70 for $Z^0 + \Upsilon$. Even after allowing for detector acceptances and efficiencies, there should be enough events to make these processes observable. In Fig. 4, we plot the invariant mass distributions $d\sigma/dM_{W\Upsilon}$ (summed over $W^{\pm}$) and $d\sigma/dM_{Z\Upsilon}$. They peak at only a few GeV above the thresholds at 89.8 GeV for $W^{\pm} + \Upsilon$ and 100.6 GeV for $Z^0 + \Upsilon$. The cross sections for $W^{\pm} + \Upsilon$ and $Z^0 + \Upsilon$ are both dominated by the $\langle \mathcal{O}_8(^3S_1)\rangle$ term. While the color-singlet matrix element is accurately normalized by the leptonic decay width of the $\Upsilon$, there is a large uncertainty in the normalization of the color-octet matrix element. The uncertainty in the value of $\sum B\langle \mathcal{O}_8(^3S_1)\rangle$ leads to a substantial uncertainty in the normalizations of the cross sections. However, this uncertainty cancels in the ratio $\sum_{\pm} \sigma(W^{\pm} + \Upsilon)/\sigma(Z^0 + \Upsilon)$, which is predicted to be about 3 at the Tevatron and about 2 at the LHC. If a significant deviation from this prediction will be observed at the LHC, this might be evidence for an additional contribution from a heavy particle that decays into $W^{\pm} + b\bar{b}$ or $Z^0 + b\bar{b}$.

The processes of $W^{\pm} + \Upsilon$ and $Z^0 + \Upsilon$ production provide lamp-posts under which one can look for new physics. The most promising possibility is to search for a charged Higgs via the decay $H^+ \to W^+ + \Upsilon$. The decay rate of the charged Higgs into $W + b\bar{b}$ is enhanced by the Yukawa coupling of the Higgs to a virtual top quark. If the mass of the charged Higgs is in the range between 140 GeV and the $t\bar{b}$ threshold and if the Higgs mixing parameter $\tan\beta$ is small, then $W + b\bar{b}$ may be the largest single decay mode [22]. The decay rate of the charged Higgs into $W + \Upsilon$ was first calculated by Grifols, Gunion, and Mendez [23]. For small $\tan\beta$, the branching fraction $B(H^+ \to W^+ + \Upsilon)$ ranges from about $10^{-4}$ if the Higgs mass is just above the $W^+ + \Upsilon$ threshold to about $10^{-3}$ if the Higgs mass is just below the $t\bar{b}$ threshold.

In a hadron collider, most of the standard production mechanisms for a charged Higgs in the mass range below the $t\bar{b}$ threshold involve the production of an additional very massive particle [24]. The standard production mechanisms

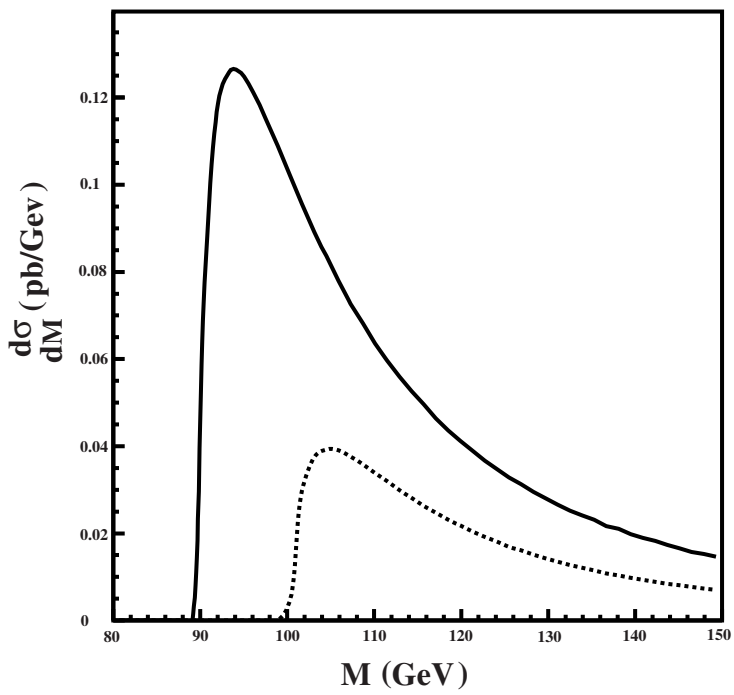


**Fig. 4.** The invariant mass distributions $d\sigma/dM_{W\Upsilon}$ (summed over $W^{\pm}$) and $d\sigma/dM_{Z\Upsilon}$ of $pp \to \Upsilon + W/Z + X$ at the LHC.

for $H^+$ include $t\bar{t}$ production followed by the decay $t \to H^+ b$, $\bar{t}H^+$ production, $W^- H^+$ production, and $H^- H^+$ production. Because of the additional very massive particle, events in which a charged Higgs decays into $W + \Upsilon$ will be easily distinguished from $W + \Upsilon$ events produced by Standard Model processes. There is one potentially significant production process for a charged Higgs that could result in events that resemble Standard Model $W + \Upsilon$ events. That process is $qb \to q'bH^+$, which proceeds through a Feynman diagram that involves a virtual $W$ boson and a virtual top quark [25].

## 5 Conclusion

The introduction of the color-octet mechanism made it possible to explain the enormous surplus in unpolarized $\psi(1S, 2S)$ production at the Tevatron. At HERA,

one still cannot definitely say whether NRQCD is working or not since NRQCD loses its predictive power in some kinematic region. High $Q^2$ leptoproduction of $J/\psi$ proposed by Fleming and Mehen might give a more concrete answer to this. Associate production of $\Upsilon$ and weak gauge bosons at the LHC might be a lamp-post under which one can probe a charged heavy resonance.

Within NRQCD, one can also predict the polarization [26] of heavy quarkonia. Polarization predictions for direct $\psi$ and $\psi'$ production at the Tevatron are already known [27]. But the first experimental result for polarized production at the Tevatron would be that of prompt $\psi$, which includes cascade effects so that one needs to include the feed-down effect. Further test of polarized quarkonium production at the Tevatron will be one of the most important tests of NRQCD in the near future.

**Acknowledgments.** The author thanks the organizers of this workshop for the invitation, E. Braaten and S. Fleming for their enjoyable collaborations on the subject discussed in Sec. 4, and B. A. Kniehl for his reading this manuscript. This work was supported in part by the Alexander von Humboldt Foundation.

## References

1. E. L. Berger and D. Jones, Phys. Rev. D **23**, 1521 (1981).
2. R. Baier and R. Rückl, Z. Phys. C **19**, 251 (1983).
3. E. Braaten and T. C. Yuan, Phys. Rev. Lett. **71**, 1673 (1993).
4. E. Braaten and M. A. Doncheski, S. Fleming and M. L. Mangano, Phys. Lett. B **333**, 548 (1994);
   D. P. Roy and K. Sridhar, Phys. Lett. B **339**, 141 (1994);
   M. Cacciari and M. Greco, Phys. Rev. Lett. **73**, 1586 (1994).
5. The CDF Collaboration, Fermilab-Conf-94/136-E (1994).
6. The CDF Collaboration, M. Mangano, in *Proceedings of the 27th International Conference on High Energy Physics*, Glasgow, Scotland, 1994, edited by P. J. Bussey and I. G. Knowles (IOP, London, 1995), and references therein; The CDF Collaboration, Phys. Rev. Lett. **79**, 572 (1997).
7. E. Braaten and S. Fleming, Phys. Rev. Lett. **74**, 3327 (1995).
8. G. P. Lepage, L. Magnea, C. Nakhleh, U. Magnea and K. Hornbostel, Phys. Rev. D **46**, 4052 (1992).
9. G. T. Bodwin, E. Braaten and G. P. Lepage, Phys. Rev. D **51**, 1125 (1995);**55**, 5853(E) (1997).
10. P. Cho, A. K. Leibovich, Phys. Rev. D **53**, 150 (1996); *ibid.* **53**, 6203 (1996).
11. M. Cacciari and M. Krämer, Phys. Rev. Lett. **76**, 4128(1996);
    J. Amundson, S. Fleming and I. Maksymyk, Phys. Rev. D **56**, 5844 (1997); M. Krämer, Nucl. Phys. B **459**, 3 (1996);
    F. Maltoni, M. L. Mangano, A. Petrelli, Nucl. Phys. B **519**, 361 (1998).
12. P. Ko, Jungil Lee and H. S. Song, Phys. Rev. D **54**, 4312 (1996); **60**, 119902(E) (1999).
13. H. Jung, G. A. Schuler and J. Terron, Int. J. Mod. Phys., A **7**, 7955 (1992);
    M. Krämer, J. Zunft, J. Steegborn, P. M. Zerwas, Phys. Lett. B **348**, 657 (1995).

14. H1 Collaboration, Nucl. Phys. B **472**, 3 (1996); ZEUS Collaboration, Z. Phys. C **76**, 599 (1997).
15. M. Beneke, I. Z. Rothstein and M. B. Wise, Phys. Lett. **B408**, 373 (1997).
16. S. Fleming and T. Mehen, Phys. Rev. D **57**, 1846 (1998).
17. H1 Collaboration, DESY-99-026 (hep-ex/9903008).
18. B. A. Kniehl and G. Kramer, Eur. Phys. J. C **6**, 493 (1999).
19. B. Cano-Coloma and M. A. Sanchis-Lozano, Nucl. Phys. B **508**, 753 (1997).
20. V. Barger, S. Fleming, and R.J.N. Phillips, Phys. Lett. B **371**, 111 (1996).
21. E. Braaten, J. Lee, and S. Fleming, Phys. Rev. D **60**, 091501 (1999).
22. S. Moretti and W.J. Stirling, Phys. Lett. B **347**, 291 (1995); Phys. Lett. B **366**, 451 (1996); E. Barradas, J.L. Diaz-Cruz, A. Gutierrez, and A. Rosado, Phys. Rev. D **53**, 1678 (1996); A. Djouadi, J. Kalinowski, and P.M. Zerwas, Z. Phys. C **70**, 435 (1996); E. Ma, D.P. Roy, and J. Wudka, Phys. Rev. Lett. **80**, 1162 (1998).
23. J.A. Grifols, J.F. Gunion, and A. Mendez, Phys. Lett. B **197**, 266 (1987); R.W. Robinett and L. Weinkauf, Mod. Phys. Lett A **6**, 1575 (1991).
24. J.F. Gunion, H.E. Haber, G.L. Kane, and S. Dawson, *The Higgs Hunter's Guide* (Addison-Wesley, Redwood City, 1990).
25. S. Moretti and K. Odagiri, Phys. Rev. D **55**, 5627 (1997).
26. E. Braaten and Y.-Q. Chen, Phys. Rev. D **54**, 3216 (1996).
27. M. Beneke and I. Z. Rothstein, Phys. Lett. B **372**, 157 (1996); M. Beneke and M. Krämer, Phys. Rev. D **55**, R5269 (1997); A. K. Leibovich, Phys. Rev. D **56**, 4412 (1997).